A novel mechanism of ribonuclease regulation: GcvB and Hfq stabilize the mRNA that encodes RNase BN/Z during exponential phase

Received for publication, October 4, 2019, and in revised form, November 13, 2019 Published, Papers in Press, November 19, 2019, DOI 10.1074/jbc.RA119.011367

Hua Chen, Angelica Previero, and Murray P. Deutscher[1]

From the Department of Biochemistry and Molecular Biology, University of Miami Miller School of Medicine, Miami, Florida 33101

Edited by Karin Musier-Forsyth

RNase BN, the *Escherichia coli* RNase Z family member, plays a limited role in tRNA metabolism, in contrast to most other organisms. However, RNase BN does act on 6S RNA, the global transcription regulator, degrading it in exponential-phase cells and maintaining it at low levels during this phase of growth. RNase BN levels decrease in stationary-phase cells, leading to elevation of 6S RNA and subsequent regulation of RNA polymerase. These findings were the first indication that RNase BN itself is growth phase–regulated. Here, we analyze the mechanism of this regulation of RNase BN. We find that RNase BN decreases in stationary phase because its mRNA becomes unstable, due primarily to its degradation by RNase E. However, in exponential-phase cells *rbn* mRNA is stabilized due to binding by the sRNA, GcvB, and the protein, Hfq, which reduce cleavage by RNase E. Because the amount of GcvB decreases in stationary phase, *rbn* mRNA is less protected and becomes increasingly unstable resulting in reduction in the amount of RNase BN. The small RNA-dependent, positive regulation of RNase BN in exponential-phase cells is the first example of this novel mechanism for RNase regulation.

Ribonucleases (RNases) are integral components of every aspect of RNA metabolism playing a central role in maturation and degradation of all RNA molecules (1, 2). However, RNases may also carry out detrimental reactions leading to the unwanted destruction of important RNAs (3). As a consequence, cells have evolved regulatory processes to control the amount and activity of individual RNases through mechanisms that have begun to be identified in recent years (3–5). In addition, it has become apparent that cells also regulate the levels of specific RNases in response to changes in environmental conditions (6). Understanding the diverse mechanisms that underlie the processes that regulate RNases is of critical importance in light of the central role of these enzymes in RNA metabolism.

RNase BN is both an endoribonuclease and a 3′ → 5′-exoribonuclease, and it is the *Escherichia coli* member of the RNase Z family of RNases (7–9). It was originally discovered based on its requirement for the maturation of certain phage T4 tRNA precursors that lack an encoded 3′-terminal -CCA sequence (10, 11), a common feature of the specificity of RNase Z family members. This raised the question of why *E. coli* contains an RNase Z homologue as all its tRNA genes already encode the -CCA sequence (12), and it strongly suggested that RNase BN serves a different function than tRNA maturation in this organism. Recently, we found that RNase BN controls the level of the global transcription regulator, 6S RNA, throughout growth of *E. coli* (13). We observed that 6S RNA remains low in exponential-phase cells because it is degraded by RNase BN and that it increases in stationary phase as the amount of RNase BN decreases (13). In addition to their importance for 6S RNA metabolism, these findings also indicated that RNase BN itself is subject to growth phase-dependent regulation.

In this paper, we identify the unusual mechanism by which RNase BN is regulated. We find that the *rbn* message and RNase BN decrease in stationary phase as much as 10-fold from their levels in exponential-phase cells. The reduction is not due to a transcriptional effect because that process appears to be unchanged in the two phases of growth. Rather, it results from the fact that the *rbn* message is much less stable in stationary-phase cells. RNase E is largely responsible for the instability of *rbn* mRNA, although RNase G can also contribute to the message decay. RNase BN protein is stable during both phases of growth, supporting the conclusion that the lower amount of RNase BN in stationary-phase cells is a consequence of the greater instability of its message. Analysis of factors that might affect *rbn* mRNA stability revealed that the protein, Hfq, and the sRNA, GcvB, act to stabilize the exponential-phase message; however, as the level of GcvB decreases in stationary-phase cells, *rbn* mRNA becomes increasingly sensitive to degradation, ultimately leading to reduction in the amount of RNase BN. *In vitro* analysis using purified components directly confirmed that GcvB binds to *rbn* mRNA in the presence of Hfq and that RNase E cleaves *rbn* mRNA. These data identify a novel mechanism for regulation of RNase BN and add to the growing list of diverse processes that control ribonucleases.

This work was supported by The National Institutes of Health Grant GM016317 (to M. P. D.). The authors declare that they have no conflicts of interest with the contents of this article. The content is solely the responsibility of the authors and does not necessarily represent the official views of the National Institutes of Health.

This article contains Table S1.

[1] To whom correspondence should be addressed: Dept. of Biochemistry and Molecular Biology, University of Miami Miller School of Medicine, P. O. Box 016129, Miami, FL 33101. Tel.: 305-243-3150; E-mail: m.deutscher@med.miami.edu.

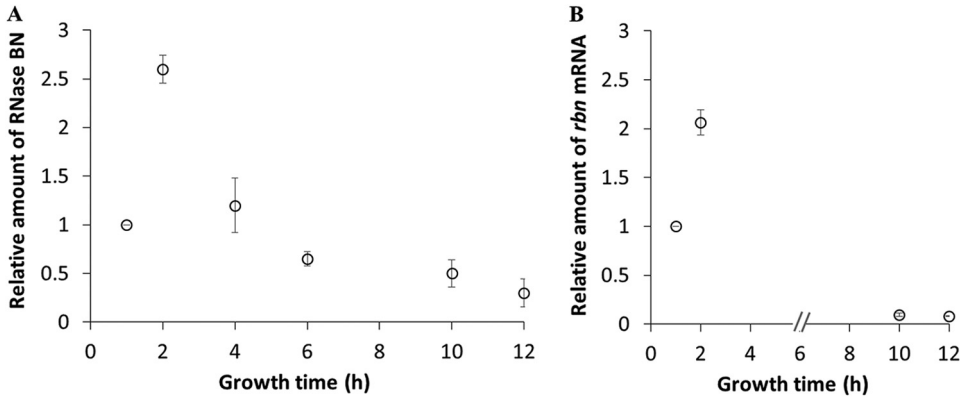

Figure 1. Accumulation of RNase BN and *rbn* mRNA throughout growth. Overnight cultures were diluted into 50 ml of YT medium and grown at 37 °C. Cells were removed at the indicated time points followed by preparation of total RNA or protein. *A,* accumulation of RNase BN protein analyzed by immunoblotting. Twenty μg of total protein was separated by 10% SDS-PAGE and subjected to Western blot analysis using anti-FLAG primary antibody as described under "Experimental procedures," and as shown in our previous work (13). *B,* accumulation of *rbn* mRNA determined by RT-qPCR. cDNA was synthesized from 1.2 μg of total RNA and subjected to RT-qPCR as described under "Experimental procedures." The amount of *rbn* mRNA was normalized by comparison with RT-qPCR of 16S RNA at each time point. The relative amount of RNase BN or *rbn* mRNA is presented compared with the corresponding 1-h sample, which was set at 1.0. The average ± S.D. from two independent experiments is presented.

Results

RNase BN is regulated by growth phase

In earlier work (13), we found that RNase BN levels decrease as cells enter stationary phase. More detailed examination of the phenomenon (Fig. 1*A*) revealed that reduction in the amount of RNase BN begins in late-exponential phase and that the overall decrease in RNase BN from its maximal level in exponential phase can be as much as 10-fold. Analysis of the amount of *rbn* mRNA (Fig. 1*B*) indicated that it also varied with growth phase in the same manner as observed for RNase BN protein. These data suggest that regulation of RNase BN is determined at the transcriptional or post-transcriptional level, rather than on translation or protein stability.

rbn mRNA transcription is the same in both growth phases

To examine how the amount of *rbn* mRNA might be regulated in exponential- and stationary-phase cells, we first determined the transcription start site in the two phases of growth using 5′-RACE[2] (Fig. 2). Based on this analysis (Fig. 2*B*), transcription of the *rbn* message initiated at the same position in both exponential- and stationary-phase cells, at an A residue located 26 nucleotides upstream of the likely initiator ATG codon (Fig. 2*A*). Examination of the nucleotide sequence upstream of the transcription start site identified putative −10 and −35 promoter sequences that were in agreement with those predicted from global transcription analysis (14, 15).

To further analyze *rbn* transcription during the two phases of growth and to examine any effects of termination, we deleted the 3′UTR beginning at the 3rd residue following the TAA termination codon. Examination of *rbn* expression revealed no difference between the WT and the Δ3′UTR strain in either exponential or stationary phase (Fig. 2*C*). In addition, a promoter fusion between the −69 to +65 region of *rbn* and *lacZ* showed little difference in β-gal activity throughout growth (Fig. 2*D*). Based on all these analyses, there is no indication that transcription of *rbn* differs between exponential- and stationary-phase cells.

rbn mRNA stability differs in the two growth phases

In light of the above findings, we sought other explanations for the dramatic reduction of *rbn* message in stationary-phase cells. To this end, we examined *rbn* mRNA stability during the two phases of growth. As shown in Fig. 3*A*, stationary phase *rbn* mRNA was much more unstable than its counterpart in exponential-phase cells, exhibiting a half-life of ~2 min compared with ~8 min for the exponential-phase message. In contrast, there was no difference in the stability of a control message encoding another RNase, that for polynucleotide phosphorylase (*pnp*) (Fig. 3*A*), indicating that instability was not a common feature of RNase mRNAs in stationary phase. Analysis of the half-life of RNase BN itself indicated that the protein was stable during both phases of growth (Fig. 3*B*). Based on these data, we conclude that the relative instability of *rbn* mRNA is a major contributor to its reduction in stationary-phase cells.

RNase E is primarily responsible for degradation of rbn mRNA

The instability of *rbn* mRNA in the stationary phase raised the question of why the message was so unstable compared with that in the exponential phase. To help answer this question, we first examined which RNase(s) might be responsible for degradation of the *rbn* mRNA. As can be seen in Fig. 4*A*, removal of the endoribonuclease, RNase E, led to dramatic stabilization of the *rbn* message, increasing its half-life from ~2 to ~10 min. However, mRNA decay still continued, although at a reduced rate suggesting the involvement of another RNase as well. In addition, as shown in Fig. 4*B*, the action of RNase E on the *rbn* message does not require its association with the RNA degradosome because deletion of the C-terminal region of RNase E, which is responsible for its association in the degradosome, had no effect on *rbn* mRNA degradation.

To examine which other RNase might participate in *rbn* mRNA degradation, we removed RNase G, a homologue of RNase E. Its removal did not affect *rbn* mRNA decay (Fig. 4*C*).

[2] The abbreviations used are: 5′-RACE, rapid amplification of cDNA end; RppH, RNA pyrophosphohydrolase; HRP, horseradish peroxidase; nt, nucleotide.

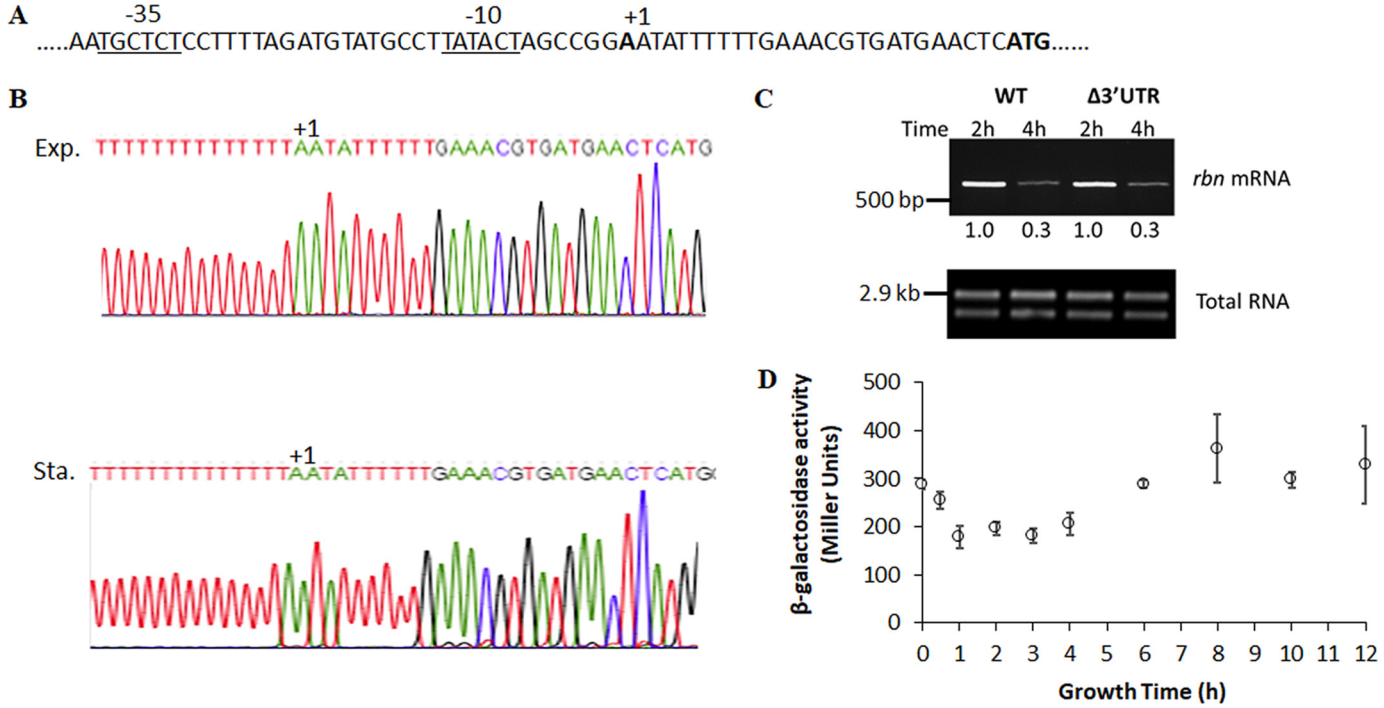

Figure 2. Analysis of transcription of *rbn* mRNA. *A,* sequence of the *rbn* promoter region. The transcription start site is labeled as +1. The predicted upstream regions at −10 and −35 are *underlined*. The putative start codon "ATG" is in *bold*. *B,* transcription start site of *rbn* mRNA. Overnight cultures were diluted into 50 ml of YT medium and grown to exponential phase (A_{600} = 0.4) and stationary phase (A_{600} = 2.0). Total RNA was isolated and subjected to 5′-RACE analysis as described under "Experimental procedures." The first nucleotide adjacent to poly(T) on the sequencing chromatograms, labeled +1, was designated as the transcription start site of *rbn* mRNA and is identical in both phases of growth. *Exp*, exponential phase; *Sta*, stationary phase. *C,* accumulation of *rbn* mRNA in Δ3′UTR mutant determined by RT-PCR. A representative experiment carried out twice with essentially identical results is shown. The *number below each lane* is the relative amount of *rbn* mRNA when compared with the 2-h sample, which was set at 1.0. The Δ3′UTR mutant was constructed by deleting nucleotides 3–93 after the stop codon of *rbn*. *D,* β-gal assay of the *rbn-lacZ* fusion. Measurement of enzyme activity of the *rbn* (−69–+65)-*lacZ* fusion was performed as described under "Experimental procedures." The average ± S.D. from three independent experiments is presented.

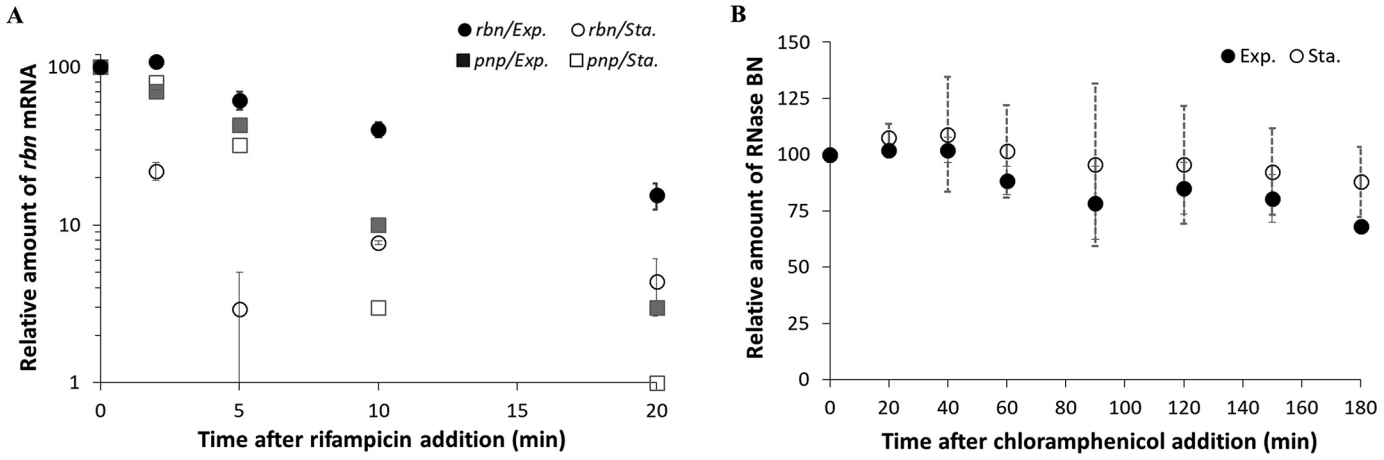

Figure 3. Stability of *rbn* mRNA and RNase BN in exponential and stationary phase. *A,* stability of *rbn* mRNA. Overnight cultures of the WT strain were diluted into 50 ml of YT medium and grown to exponential phase (A_{600} = 0.4) or stationary phase (A_{600} = 2.0). Cells were treated with 500 mg/liter rifampicin and sampled at the indicated time points. The amount of *rbn* mRNA was determined by RT-qPCR as described under "Experimental procedures" using 1.2 μg of total RNA and was normalized by comparison with RT-qPCR of 16S RNA. The stability of *pnp* mRNA, determined by RT-PCR, is used as a control. *B,* stability of RNase BN protein analyzed by immunoblotting. Exponential phase (A_{600} = 0.4) and stationary-phase cells (A_{600} = 2.0) containing chromosomal FLAG-tagged *rbn* were treated with 400 mg/liter of chloramphenicol and harvested at the indicated time points. Twenty μg of total protein was separated by 10% SDS-PAGE and was subjected to Western blotting using anti-FLAG primary antibody. The average ± S.D. from two independent experiments is presented.

However, in the absence of both RNase E and RNase G, *rbn* mRNA was essentially stable in stationary-phase cells (Fig. 4*D*). These data indicate that RNases E and G, and primarily RNase E, are responsible for degradation of the *rbn* mRNA in stationary-phase cells.

Hfq affects rbn mRNA stability in exponential phase

The major difference in *rbn* mRNA stability between exponential- and stationary-phase cells raised the question of whether trans-acting factors might be differentially affecting the message in the two phases of growth. To address this point,

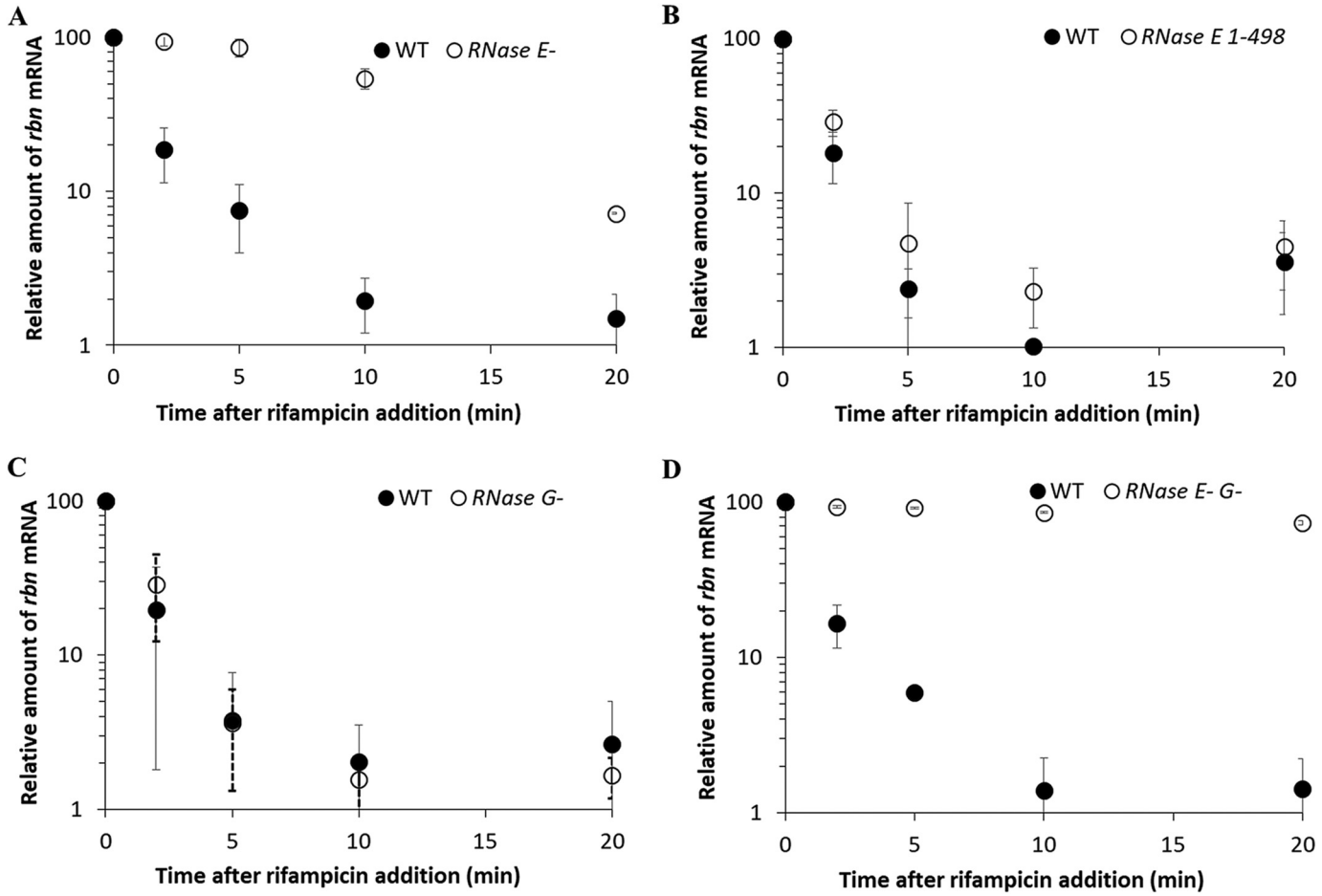

Figure 4. Roles of RNase E and RNase G in *rbn* mRNA stability. *WT*, temperature-sensitive RNase E$^-$ single mutant cells (*A*) and RNase E$^-$G$^-$ double mutant cells (*D*) were grown to early stationary phase (A_{600} = 1.5) at 30 °C before shifting to 42 °C and incubating an additional 20 min to inactivate RNase E. *WT*, RNase E 1–498 mutant cells (*B*) and RNase G$^-$ mutant cells (*C*) were continuously grown to stationary phase (A_{600} = 2.0) at 37 °C. All cultures were treated with 500 mg/liter rifampicin, and samples were removed at the indicated time points. The relative amount of *rbn* mRNA compared with that at the time of rifampicin addition was determined by RT-PCR is described under "Experimental procedures" using 1.2 μg of total RNA. The average ± S.D. from two independent experiments is presented.

we eliminated several factors known to affect mRNA stability and determined whether their removal affected *rbn* mRNA. We first examined polyadenylation catalyzed by poly(A) polymerase. As is shown in Fig. 5, *A* and *D*, mutation of the *pcnB* gene encoding poly(A) polymerase (16, 17) did not affect the stability of *rbn* mRNA in either exponential or stationary phase indicating that polyadenylation is not involved in the differential stability of this message. Removal of RNA pyrophosphohydrolase (RppH) by mutation of the *rppH* gene (18) led to stabilization of the *rbn* message in both exponential and stationary phase (Fig. 5, *B* and *E*); however, because there was no significant difference in the effect of RppH removal during the two phases of growth, it is unlikely that RppH plays any role in the differential stability of the *rbn* message in exponential and stationary phase. Stabilization of mRNA upon removal of RppH is to be expected as this enzyme facilitates mRNA degradation dependent on RNase E (18).

In contrast to the above findings, removal of the RNA chaperone, Hfq, differentially affected the stability of *rbn* mRNA in the two phases of growth (Fig. 5, *C* and *F*). In stationary-phase cells, *rbn* mRNA was equally unstable irrespective of whether Hfq was present or not (Fig. 5*F*). However, in exponential-phase cells, removal of Hfq dramatically destabilized the *rbn* message, reducing its half-life from ~7 to ~1 min (Fig. 5*C*) to a level similar to that seen in stationary-phase cells (Fig. 5*F*). These data suggest that the presence of Hfq stabilizes *rbn* mRNA in exponential phase, but not in stationary-phase cells, and as a consequence, the mRNA has different stability during the two phases of growth.

Hfq elevates the amount of RNase BN in exponential phase

To further examine the role of Hfq, we determined how its removal affected the actual amount of *rbn* mRNA and RNase BN. As shown in Fig. 6*A*, the absence of Hfq reduced the amount of *rbn* mRNA in exponential-phase cells to 34% that in WT cells (compare at A_{600} = 0.5). Concomitantly, the amount of RNase BN in the exponential phase was also reduced to ~30% that in WT cells (Fig. 6*B*). These findings confirm that the presence of Hfq is important for maintaining RNase BN at higher levels in exponential phase compared with stationary-phase cells.

Small RNAs play a role in maintaining RNase BN levels

Hfq is known to promote binding of sRNAs to complementary mRNAs (19), which raised the possibility that stabilization of the exponential phase *rbn* message by Hfq might also involve

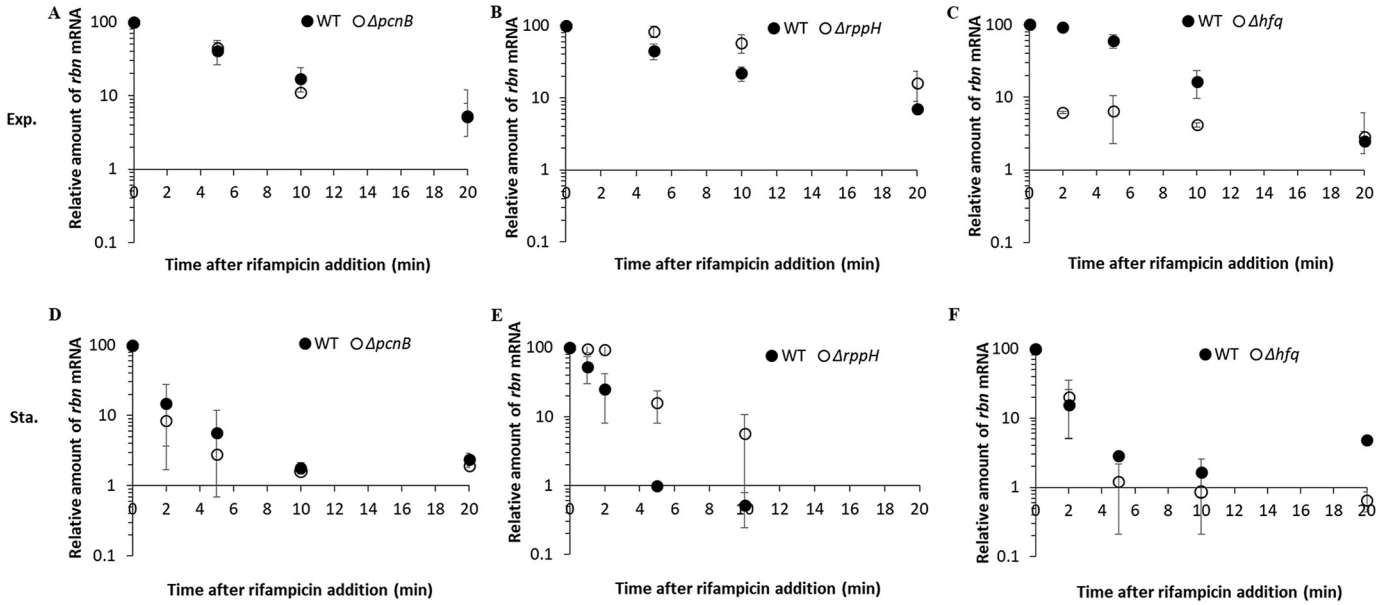

Figure 5. Examination of protein factors that affect *rbn* mRNA stability. *A–C,* effect of PAPI, RppH, and Hfq on *rbn* mRNA stability in exponential phase (*Exp.*). *D–F,* effect of PAPI, RppH, and Hfq on *rbn* mRNA stability in stationary phase (*Sta.*). Overnight cultures of the different strains were diluted into 50 ml of YT medium and grown to exponential phase (A_{600} = 0.4) or stationary phase (A_{600} = 2.0). Cells were treated with 500 mg/liter rifampicin and harvested at the indicated time points. The relative amount of *rbn* mRNA compared with that at the time of rifampicin addition was determined by RT-PCR as described under "Experimental procedures" using 1.2 μg of total RNA. The average ± S.D. from two independent experiments is presented.

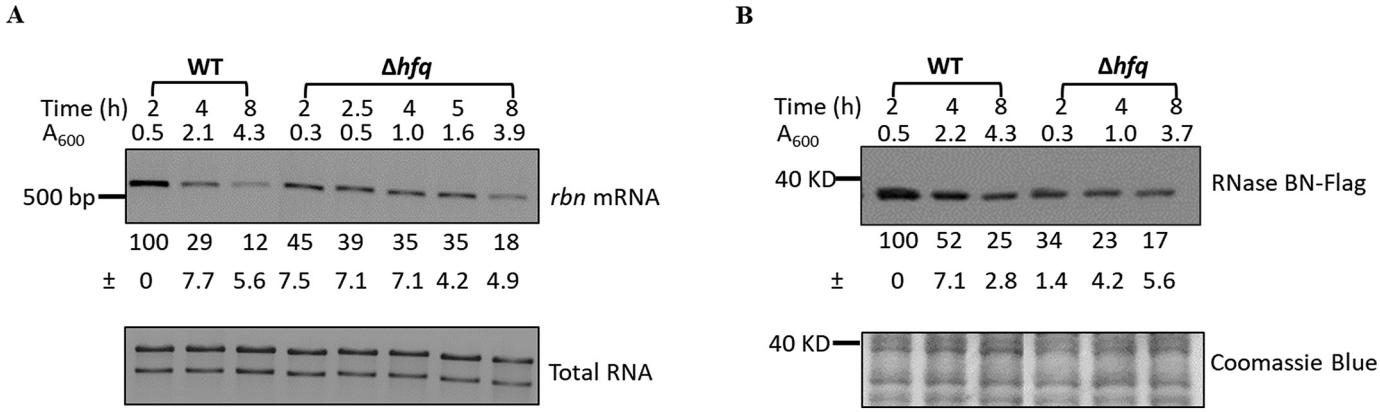

Figure 6. Effect of Hfq on the accumulation of *rbn* mRNA and RNase BN. Overnight cultures were diluted into 100 ml of YT medium, and cells were harvested at the indicated time points. Total RNA or protein was prepared as described under "Experimental procedures" and subjected to RT-PCR or immunoblotting analysis. *A,* accumulation of *rbn* mRNA in WT and Δ*hfq* strains. cDNA was synthesized using 1.2 μg of total RNA for RT-PCR. Equal amounts of total RNA were added to each lane. *B,* accumulation of RNase BN in WT and Δ*hfq* strains. Twenty μg of protein was separated by 10% PAGE and subjected to immunoblotting analysis. Coomassie Blue staining was used for the loading control. A representative experiment carried out twice with essentially identical results is shown. The relative amount of *rbn* mRNA or RNase BN protein is indicated with an average ± S.D. from the two biological replicates by comparing to the 2-h sample, which was set at 100.

an sRNA molecule that associates with *rbn* mRNA. This led us to examine whether any known sRNAs contained sequences that would lead them to bind tightly to *rbn* mRNA and were also present at higher levels in the exponential phase than in the stationary phase, a requirement for a molecule expected to stabilize the exponential phase *rbn* message. The results of this analysis, using IntaRNA (20), are shown in Table 1. Multiple sRNAs were found to fit the first criterion of having the potential to bind tightly to *rbn* mRNA. In addition, several are present at higher levels in exponential-phase cells than in stationary-phase cells. None of these interactions had been predicted previously, although very recently *rbn* mRNA was found among messages pulled down in a GcvB MAPS experiment (21). Four of the sRNAs (RyjB, GcvB, GlmZ, and Spf), which are present at

Table 1
sRNA candidates that interact with *rbn* mRNA

sRNA	Size	Position of base pairing on *rbn*[a]	Energy[b]	Expression[c]	Refs.
	nt		*kcal*		
RyjB	90	796–818	−15.7	E > S	43
RseX	91	581–613	−15.6	Unknown	44
GcvB	205	76–125	−13.3	E > S	24
GlmZ	172	254–282	−12.6	E > S	24
RprA	105	1055–1097	−11.8	S > E	24, 45
RyeB	121	496–544	−9.6	S > E	45
SraB	169	52–98	−9.2	S > E	24
SroB	82	29–44	−8.5	S > E	46
Spf	109	582–594	−7.8	E > S	47

[a] Transcription start site is position 1. Coding region begins at position 27.
[b] Position of base pairing and the energy of *rbn*-sRNA hybrid are predicted by IntaRNA.
[c] Expression is based on published data. E is exponential phase, and S is stationary phase.

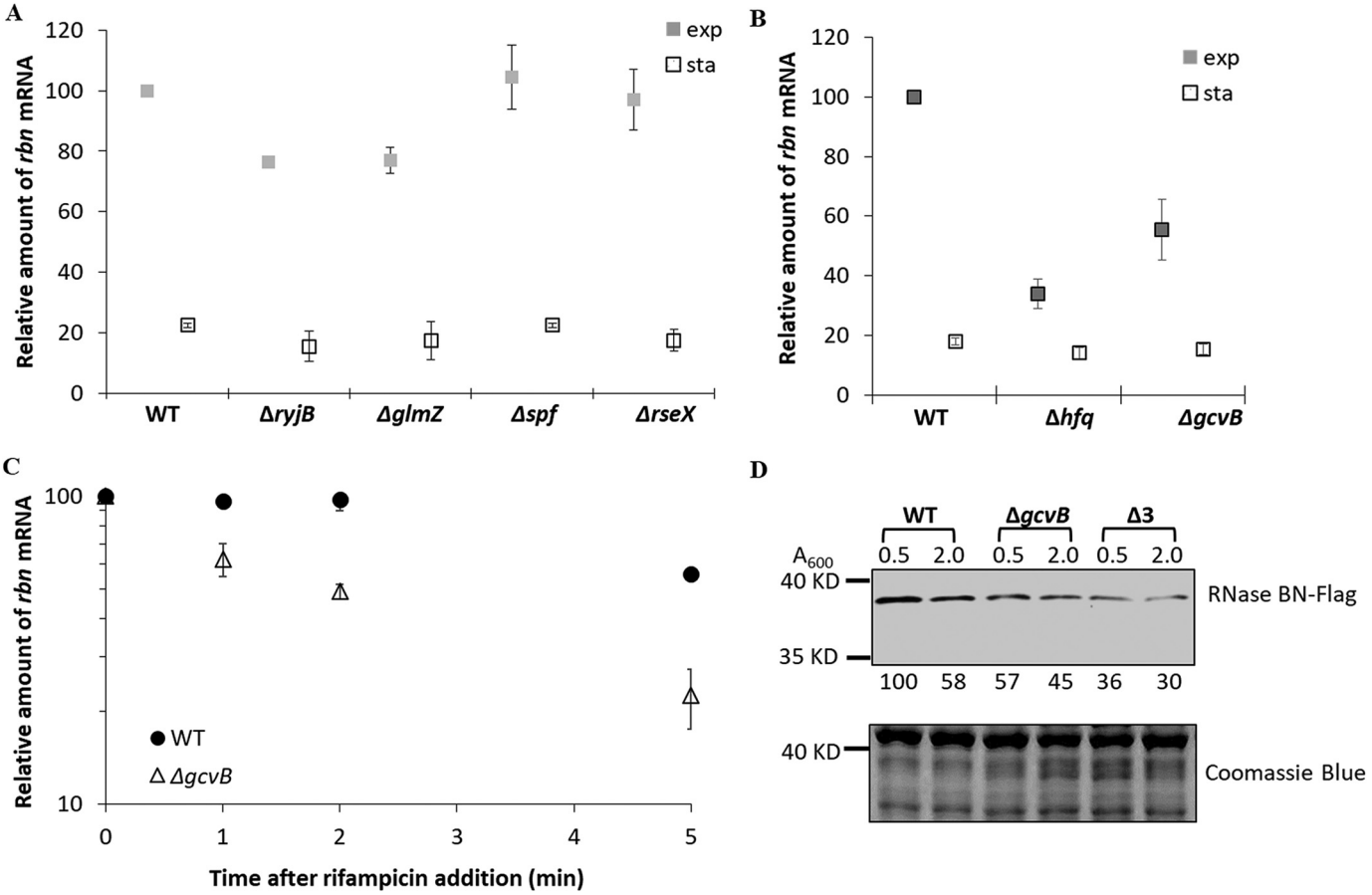

Figure 7. Effect of GcvB on *rbn* mRNA and RNase BN. *A,* effect of four small sRNAs (RyjB, GlmZ, Spf, and RseX) on the accumulation of *rbn* mRNA. *B,* effect of GcvB on the accumulation of *rbn* mRNA. Overnight cultures of wildtype (*WT*), Δ*hfq,* and Δ*gcvB* strains were diluted into 50 ml of YT medium. Cells were removed at the indicated growth stages monitored by absorbance measurement at 600 nm (*exp*, A_{600} = 0.5; *sta*, A_{600} = 2.0). The relative amount of *rbn* mRNA was determined by RT-PCR using 1.2 μg of total RNA, and it was quantified by setting the WT exponential phase sample to 100. The average ± S.D. from two independent experiments is presented. *C,* effect of GcvB on the stability of *rbn* mRNA. Overnight cultures of WT and Δ*gcvB* strains were diluted into 50 ml of YT medium and grown to exponential phase (A_{600} = 0.5). Cells were treated with 500 mg/liter rifampicin, and samples were removed at the indicated time points. The amount of *rbn* mRNA was determined by RT-PCR using 1.2 μg of total RNA. The average ± S.D. from two independent experiments is presented. *D,* accumulation of RNase BN in the Δ*gcvB* strain and the triple knockout strain (Δ3) lacking GcvB, RyjB, and GlmZ. Cells containing chromosomal FLAG-tagged *rbn* were harvested at the indicated time points. Twenty μg of total protein was separated by 10% SDS-PAGE and subjected to Western blotting using anti-FLAG primary antibody. Coomassie Blue staining was used as the loading control. A representative experiment carried out twice with essentially identical results is shown. The *number below each lane* is the relative amount of RNase BN protein when compared with the WT sample at A_{600} = 0.5, which was set at 100.

higher levels in the exponential phase, and RseX, which displays high complementarity to *rbn* mRNA, were chosen for study in more detail. Each of the RNAs was eliminated by mutation, and the effect of their removal on the amount of exponential phase *rbn* mRNA was determined. The absence of RseX or Spf had essentially no effect, although removal of RyjB or GlmZ had a small effect, lowering the amount of *rbn* mRNA present ~20% compared with the parental strain containing the sRNAs (Fig. 7*A*).

However, the absence of GcvB led to a major effect on RNase BN. As shown in Fig. 7*B*, the absence of GcvB led to an ~50% reduction in exponential-phase cells in the amount of *rbn* mRNA compared with WT, somewhat less than that seen upon removal of Hfq. In stationary-phase cells, the level of *rbn* mRNA was unaffected by removal of GcvB, and it remained below 20% that in WT exponential-phase cells (Fig. 7*B*). Moreover, the absence of GcvB reduced *rbn* mRNA half-life from >5 to 2 min (Fig. 7*C*). The absence of GcvB also resulted in a reduction in the amount of RNase BN in exponential phase (Fig. 7*D*), slightly less than that observed in the Δ*hfq* strain (Fig. 6*B*). These data strongly support the conclusion that GcvB works in concert with Hfq to stabilize *rbn* mRNA in exponential-phase cells, leading to a higher level of RNase BN.

Because the reduction of RNase BN in the Δ*gcvB* strain was not quite as much as that in the Δ*hfq* strain, we inquired whether removal of additional sRNAs might enhance the effect. To examine this point, we generated a strain lacking RyjB and GlmZ, in addition to GcvB (termed Δ3), as removal of these two sRNAs did lead to a small reduction of *rbn* mRNA (see above). As shown in Fig. 7*D*, the amount of RNase BN was reduced even further in the Δ3 strain, to a level essentially the same as obtained upon removal of Hfq (Fig. 6*A*). This finding suggests that other sRNAs also may contribute to stabilization of *rbn* mRNA in exponential phase.

GcvB levels decrease in stationary-phase cells

The data presented indicate that Hfq and GcvB together stabilize *rbn* mRNA in exponential-phase cells thereby maintaining RNase BN at higher levels during this phase of growth. A corollary of this conclusion is that Hfq, GcvB, or both should

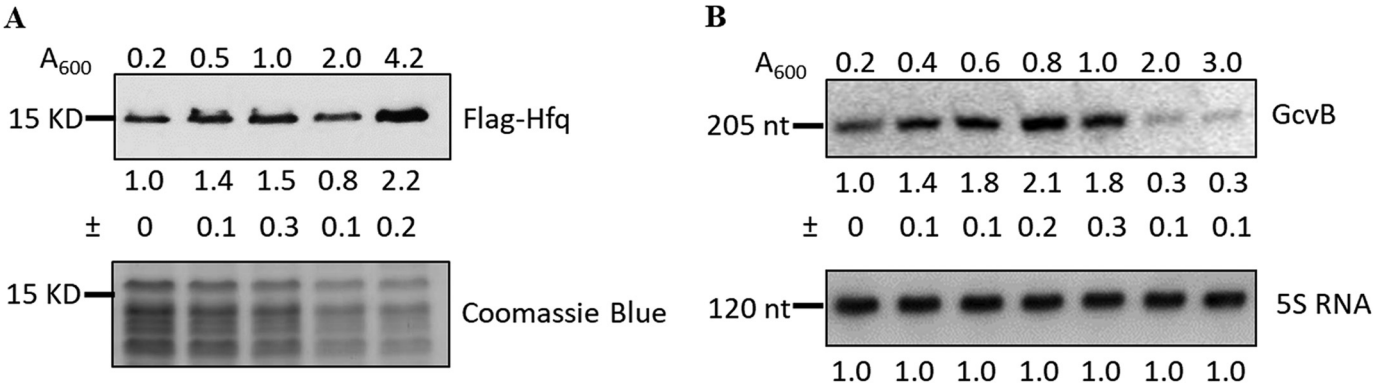

Figure 8. Accumulation of Hfq and GcvB throughout growth. *A,* accumulation of Hfq. Overnight cultures of the WT strain carrying chromosomal 3×FLAG-tagged *hfq* was diluted into 100 ml of fresh YT medium, and cells were removed at the indicated time points. Ten μg of total protein was resolved by 15% SDS-PAGE and subjected to immunoblotting using antibody directly against the FLAG tag. Coomassie Blue staining was used as the loading control. *B,* accumulation of GcvB RNA. Fifteen μg of total RNA was separated by 6% urea-PAGE and subjected to Northern blot analysis using probes specific for GcvB and 5S RNA. A representative experiment carried out twice with essentially identical results is shown. The relative amount of Hfq or GcvB is indicated with average ± S.D. from the two biological replicates by comparing to the sample at A_{600} = 0.2, which was set at 1.0.

decrease in stationary-phase cells, and this is what renders *rbn* mRNA more unstable leading to the lower amount of RNase BN. Data in the literature have been unclear on Hfq levels in the two phases of growth (22, 23), whereas GcvB is thought to be present at decreased levels in stationary phase (24). Therefore, it was deemed important to determine the levels of the two factors in our strains under our growth conditions. To this end, we analyzed the amount of Hfq and GcvB throughout growth. These data are presented in Fig. 8.

As shown in Fig. 8*A*, we find that Hfq levels increased about 2-fold as cells progressed from early exponential phase through stationary phase. In contrast, GcvB first increased in exponential phase, but then decreased dramatically (as much as 7-fold) in stationary phase (Fig. 8*B*). Based on these findings, it is likely that reduction in the amount of GcvB is responsible for destabilizing *rbn* mRNA and, ultimately, for lowering the level of RNase BN in stationary-phase cells.

GcvB binds rbn mRNA

The data presented are most consistent with the conclusion that Hfq and GcvB bind to *rbn* mRNA and protect against cleavage by RNase E due to the complementarity of GcvB to various regions of the *rbn* message (Fig. 9, *A–C*). Three regions of complementarity were identified with the strongest binding expected to be in the region between residues 76 and 125 of *rbn* mRNA (Fig. 9*C*) within the coding region of the message. To directly determine whether GcvB binds to *rbn* mRNA, a gel-shift analysis was carried out. Purified GcvB was incubated with a 5′-labeled fragment of *rbn* mRNA encompassing residues 1–165 that contains the regions complementary to GcvB (Fig. 9*D*). As can be seen, GcvB, by itself, did not interact with the *rbn* message under these assay conditions (*lanes 2–4*), although binding could be observed at 10-fold higher concentrations of *rbn* mRNA (Fig. 9*E*), indicating a direct interaction between the two RNAs. Upon addition of Hfq, under the conditions of Fig. 9*D*, two slower migrating bands of *rbn* mRNA were observed, one that formed in the presence of Hfq alone (*lane 5*) and a second band generated in the presence of both Hfq and GcvB (*lanes 6–8*). The latter band increased with increasing amounts of GcvB, whereas the amount of the *rbn* mRNA–Hfq binary complex decreased, suggesting that addition of GcvB converts the binary complex to one containing all three components. This conclusion was supported by destruction of both complexes upon incubation with proteinase K (Fig. 9*D*, *lanes 9–12*), indicating that each complex contained Hfq. Interestingly, the binary complex of *rbn* mRNA and Hfq migrates more slowly than the ternary complex that also contains GcvB. This observation suggests that Hfq, by itself, may bind at multiple positions on the message and that the addition of GcvB narrows the binding to regions of complementarity between the mRNA and the sRNA. Moreover, these data also show that Hfq greatly stimulates binding of GcvB to the *rbn* mRNA.

RNase E cleaves rbn mRNA

To directly determine whether RNase E cleaves the *rbn* message and to identify the positions of cleavage, purified RNase E was incubated with the 165-nt *rbn* mRNA fragment, and the products were analyzed by primer extension (Fig. 9*F*). RNase E cleaved the mRNA fragment at multiple positions along the mRNA sequence. Three of the cleavages, at nt 85, 96, and 103, were within the region of greatest complementarity to GcvB (Fig. 9*C*). Strong, longer extension products (noted by *arrows* in Fig. 9*F*) also were observed, indicating that additional cleavages closer to the 5′ end of the message also occur *in vitro*, but their exact positions could not be determined by this method due to poor resolution of the ladder in this region of the gel. To look more closely at these cleavages, the 5′-^{32}P-labeled mRNA fragment was used as the substrate, and the products were analyzed by gel electrophoresis (Fig. 9*G*). Multiple bands were observed, confirming that RNase E cleaves at several positions near the 5′ end of the message fragment (Fig. 9*G*, *lane 2*). It should be noted that this analysis only detects cleavage products that retain the labeled 5′ end. Nevertheless, the data in Fig. 9, *F* and *G*, clearly indicate that RNase E cleaves *rbn* mRNA at multiple specific sites.

The analysis in Fig. 9*G* could also be used to assess whether GcvB and/or Hfq protected the mRNA fragment against RNase E cleavage. Addition of GcvB had no effect on cleavage by RNase E (Fig. 9*G*, *lane 3*), but the presence of Hfq alone (*lane 4*) or Hfq and GcvB (*lane 5*) completely protected the mRNA.

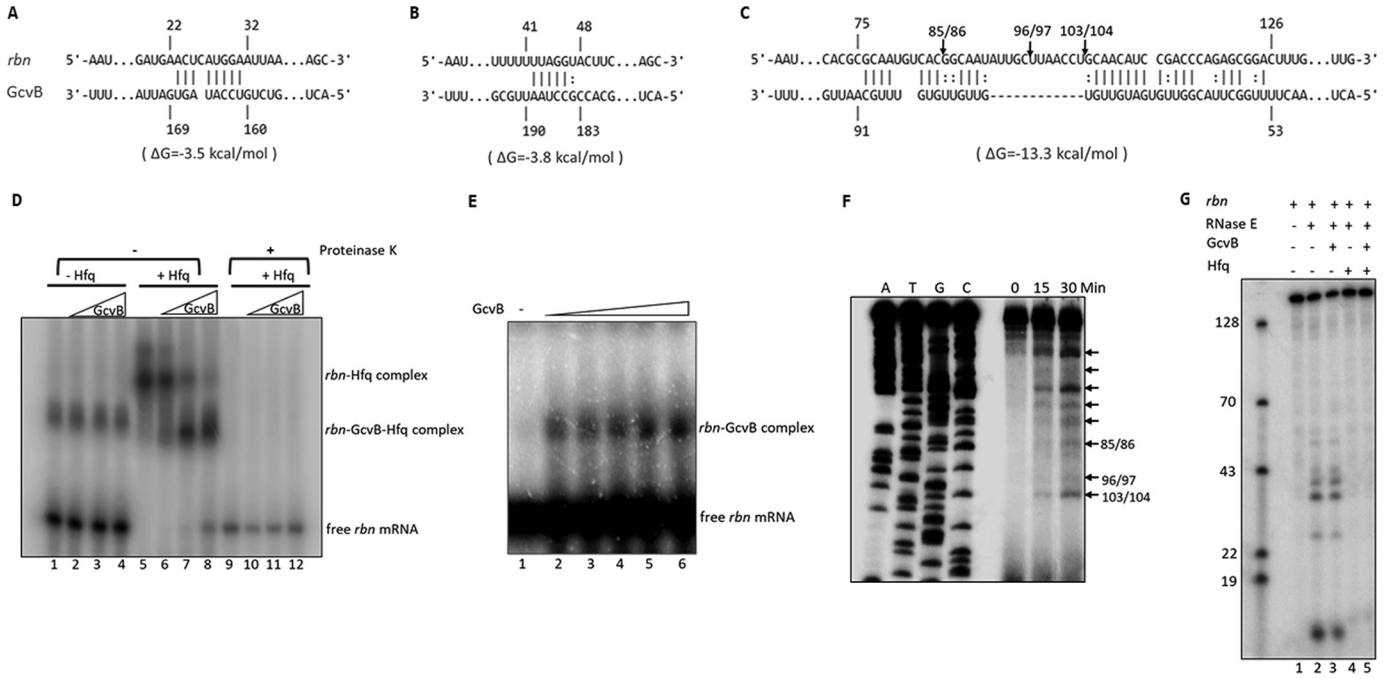

Figure 9. *In vitro* interaction of GcvB with *rbn* mRNA and cleavage by purified RNase E. *A–C,* predicted base pairing between GcvB and three regions of the 5′ 165-nt fragment of *rbn* mRNA using the IntaRNA program. Numbering of nucleotides on *rbn* mRNA and GcvB is relative to the transcription start site of each RNA. *Arrows* indicate sites of cleavage by RNase E determined by the primer extension assay shown in *E*. *D,* interaction of GcvB with *rbn* mRNA. 5′-Labeled *rbn* fragment (0.1 pmol) and 0.4 pmol (*lanes 2, 6,* and *10*), 0.8 pmol (*lanes 3, 7,* and *11*), or 1.6 pmol (*lanes 4, 8,* and *12*) of GcvB were incubated with or without purified Hfq in a 10-μl reaction. For reactions in *lanes 9–12,* 10 μg of proteinase K was added following complex formation to remove Hfq. Samples were analyzed on 5% native polyacrylamide gels. A representative experiment carried out twice with essentially identical results is shown. *E,* interaction of GcvB with *rbn* mRNA in the absence of Hfq. 5′-Labeled *rbn* fragment (1 pmol) was incubated with 1, 2, 4, 8, or 16 pmol of GcvB (*lanes 2–6,* respectively) in a 20-μl reaction. *F,* analysis of RNase E cleavage sites on *rbn* mRNA. The *rbn* fragment (1–165) was synthesized by *in vitro* transcription and digested with purified RNase E (N-terminal protein, 1–498). Digestion products were subjected to primer-extension analysis as described under "Experimental procedures." *Arrows* indicate all time-dependent cleavage products. The positions of the three cleavage sites within the region of highest complementarity to GcvB are numbered based on the sequence ladders. *G,* effect of GcvB and Hfq on *in vitro* cleavage of *rbn* mRNA by RNase E. Reaction mixtures were set up as described under "Experimental procedures." Reaction mixtures lacking RNase E were first incubated for 20 min at 37 °C, followed by addition of RNase E and additional incubation for 15 min. Cleavage products were analyzed by 8% urea-PAGE. A mixture of 5′-labeled DNA oligonucleotides was used to evaluate the size of cleavage products. *D–G,* representative experiments carried out twice with essentially identical results are shown.

Unfortunately, because Hfq binds strongly to the message *in vitro* by itself (Fig. 9*D*), and thereby protects against RNase E action (Fig. 9*G*, *lane 4*), we were unable to confirm the role of GcvB identified *in vivo* by this *in vitro* analysis. Nevertheless, taken together these data confirm the *in vivo* findings that GcvB binds to *rbn* mRNA and that the message is a substrate of RNase E.

Discussion

The studies presented here provide a clear explanation for the growth phase-dependent reduction of RNase BN as cells progress from exponential to stationary phase. Thus, we found the following: 1) *rbn* mRNA is present at lower levels in stationary-phase cells and that this reduction is due to greater instability of the message at this stage of growth; 2) primarily RNase E, but also RNase G, are responsible for *rbn* mRNA degradation; 3) the sRNA, GcvB, and the protein Hfq stabilize *rbn* mRNA in exponential-phase cells, and this stabilization can be reversed upon elimination of either of these factors by mutation; 4) GcvB binds and RNase E cleaves *rbn* mRNA *in vitro*; and 5) GcvB levels normally decrease in stationary-phase cells that leads to the instability of *rbn* mRNA and ultimately to the reduction in RNase BN. This regulatory process joins the regulation of RNase R by tmRNA (25) as the second example in which an sRNA regulates an RNase. However, in the former case, regulation was at the level of RNase R protein stability (25), rather than on mRNA stability, as described here. These findings further emphasize the importance of RNase regulation both for limiting unwanted deleterious reactions and for altering RNase activity in response to changes in environmental conditions.

Although GcvB was the primary small RNA to affect *rbn* mRNA stability, it is likely that other sRNAs may also contribute to some degree. First, removal of RyjB or GlmZ, two other sRNAs with complementarity to *rbn* message, led to ~20% reductions in *rbn* mRNA in exponential phase; and second, elimination of RyjB and GlmZ, in addition to GcvB, resulted in a greater reduction in the amount of RNase BN in exponential-phase cells (Fig. 7*C*). Inasmuch as Hfq acts together with multiple sRNAs, the finding of a greater reduction of RNase BN upon its elimination than that of GcvB alone also supports the involvement of other sRNAs in stabilizing *rbn* mRNA. We do not yet understand why multiple sRNAs would each regulate *rbn* mRNA stability, but it raises the possibility that diverse, independent signals can affect RNase BN levels. Further work will be necessary to clarify this point.

Hfq mediates many interactions between sRNAs and mRNAs leading to a wide range of negative and positive regulatory effects on the mRNA targets (19). To date, only a handful

of examples have been identified in which binding of a small RNA has been found to stabilize an mRNA against RNase action (26, 27), and this is the only example in which the target mRNA itself encodes an RNase. Inasmuch as the RNase product, in this case RNase BN, has the potential to affect many RNA molecules, this regulatory process could be of widespread significance to cellular metabolism. In fact, we have already found that RNase BN regulates 6S RNA abundance keeping its level low in exponential-phase cells, but allowing it to increase in stationary phase (13). Because 6S RNA is an important regulator of σ70-containing RNA polymerase, acting to reduce its activity in stationary-phase cells (28), the regulation of RNase BN could have significant consequences for gene expression.

It is somewhat surprising that GcvB is involved in target activation of RNase BN. GcvB is an important sRNA that targets a large number of genes in bacteria (29), including many involved in amino acid metabolism (30). Global transcription analysis revealed that the amounts of most known GcvB targets are higher in stationary phase than in exponential phase (31), implying that GcvB most commonly acts as a repressor of gene expression in exponential-phase cells, and that this repression ceases as GcvB levels decrease in stationary phase. Hence, its action on RNase BN in which it stabilizes *rbn* mRNA and thereby elevates the RNase in exponential phase is quite unusual. Interestingly, GcvB itself is stabilized and regulated by Hfq (32), but whether this plays any role in the reduction in GcvB in stationary phase is not known. Nevertheless, the intertwined regulatory circuits that encompass RNase BN, 6S RNA, σ70-RNA polymerase, Hfq, and GcvB, and how they affect gene expression in exponential and stationary-phase cells, will undoubtedly provide a wealth of fascinating information.

Experimental procedures

Materials

[γ-^{32}P]ATP was purchased from PerkinElmer Life Sciences. T4 polynucleotide kinase, terminal transferase, Moloney murine leukemia virus–reverse transcriptase, RNase-free DNase I, and Taq2× Master Mix were products of New England Biolabs. DNA Clean & Concentrator™ was obtained from Zymo Research. QIAquick™ gel extraction kit was from Qiagen. TA cloning kit with PCR™ 2.1 vector and MEGAshortscript™ T7 transcription kit were from Thermo Fisher Scientific. SsoAdvanced™ Universal SYBR® Green Supermix and 0.45- and 0.2-μm nitrocellulose membranes were from Bio-Rad. Anti-mouse IgG HRP conjugate and calf intestinal alkaline phosphatase were obtained from Promega Corp. Thermo Sequence Cycle Sequencing kit was from Affymetrix Inc. SequaGel® urea gel system for denaturing urea-polyacrylamide gels was from National Diagnostics. Oligonucleotides, anti-FLAG M2 mAbs, and Amicon® ultracentrifugal units were obtained from Sigma. Nytran™ SPC nylon transfer membrane was from GE Healthcare. ExpressHyb™ hybridization solution was obtained from Clontech. All other chemicals were reagent grade.

Bacterial strains and growth conditions

Bacterial strains used in this study were derivatives of WT *E. coli* K-12 strain MG1655 (Seq) *rph*$^+$. The WT strain with chromosomal FLAG-tagged *rbn* was constructed in previous work (13). The WT strain with chromosomal FLAG-tagged *hfq* was a gift from Dr. Chaitanya Jain's laboratory (University of Miami). Knockout strains of RppH, PAPI, Hfq, and lacZ were provided by Dr. Kenneth Rudd (University of Miami). The knockout strain lacking RNase G, the mutant strain RNase E(1–498), and the temperature-sensitive mutant strain RNase E$^-$ were from laboratory stocks. Null strains lacking the small noncoding RNAs (GlmZ, RyjB, RseX, GcvB, and Spf) and the *rbn*-Δ3′UTR strain were constructed by recombining (33) using the primers listed in Table S1. The triple knockout strain lacking GcvB, GlmZ, and RyjB (termed Δ3) and the double knockout strain lacking *rbn* and *lacZ* were constructed by transduction using phage P1 *vir*. The strains containing chromosomal FLAG-tagged *rbn* in the background of Δ*hfq*, Δ*gcvB*, and Δ3 were also constructed by transduction using phage P1 *vir*.

Cells were grown in YT medium (Bacto-tryptone 8 g/liter, yeast extract 5 g/liter, sodium chloride 5 g/liter) at 30 or 37 °C. To inactivate RNase E, cultures grown at 30 °C were shifted to 42 °C and incubated for 20 min. Antibiotics, when present, were at the following concentrations: kanamycin, 25 μg/ml; ampicillin, 100 μg/ml; chloramphenicol, 17 μg/ml.

β-Gal assay

The *rbn* fragment −69 to +65 was amplified from chromosomal DNA of the WT strain using primers HC35 and HC36 in Table S1. PCR products were digested and ligated into the BamHI and HindIII restriction sites of the low-copy vector pLACZY1a (a gift from Dr. Chaitanya Jain) (34). The construct were introduced into *E. coli* strain MG1655 (Seq) *rph*$^+$ Δ*rbn* Δ*lacZ*.

Overnight cultures were diluted 1:200 into 200 ml of YT medium containing 100 μg/ml ampicillin. Cells were removed at different time points as indicated in Fig. 2*D*, followed by centrifuging at 4 °C. Cell pellets were resuspended in buffer Z (60 mM Na_2HPO_4, 40 mM NaH_2PO_4, 10 mM KCl, 1 mM $MgSO_4$, 50 mM β-mercaptoethanol). β-Gal activity was measured, as described previously (35), and was presented as Miller units by calculating the value $1000 \times ((OD_{420} - 1.75 \times OD_{550}))/(t \times V \times OD_{600})$, where t is time of the reactions in minutes, and V is volume of the cultures in milliliters.

RNA decay

Overnight cultures were diluted 1:200 into fresh YT medium and grown to exponential phase (A_{600} = 0.4) or stationary phase (A_{600} = 2.0) followed by treatment with 500 μg/ml rifampicin. Equal amounts of cells were removed for the zero-time sample after 75 s of rifampicin addition to allow complete inhibition of new transcription, and immediately mixed with ice-cold stop solution (95% ethanol, 5% phenol). Additional samples were removed at different time points as indicated in the figure legends. Changes in *rbn* mRNA levels were determined by quantitative RT-PCR (RT-qPCR) or RT-PCR.

RNA extraction, RT-PCR, and RT-qPCR

Total RNA was prepared using the hot phenol method described previously (36), and the RNA concentration was determined by UV spectroscopy. DNase I-treated RNA (1.2 μg)

was reverse-transcribed with the primers HC08 (*rbn* gene-specific primer), HC05 (16S RNA gene-specific primer), and HC12 (*pnp* gene-specific primer), using Moloney murine leukemia virus reverse transcriptase. The resulting cDNA was amplified by PCR using primers HC11 and HC02 to amplify *rbn* or using primers HC13 and HC14 to amplify *pnp*. PCR products were loaded on a 1.0% agarose gel and visualized using the Biodoc-it imaging system (UVP). The sequences of oligonucleotides are listed in Table S1.

To perform RT-qPCR analysis, 5 μl of 1:100 diluted cDNA was added to 20 μl of qPCR mixture together with 10 μl of SSoAdvanced^{TM} universal SYBR® Green supermix and 0.5 μM gene-specific primers for *rbn* (HC09 and HC10) or 16S RNA (HC06 and HC07) as listed in Table S1. The amplification was carried out using MiniOpticon^{TM} real-PCR system (Bio-Rad), and the data were analyzed using CFX Manager^{TM} software (version 3.1).

5′-RACE assay

5′-RACE assay was performed as described previously (37). cDNA was synthesized from 2 μg of total RNA using an *rbn*-specific primer and was purified using DNA Clean & Concentrator^{TM}, followed by the addition of a poly(A) tail in a 20-μl reaction containing 2 μl of 10× reaction buffer, 2 μl of 10× $CoCl_2$ (2.5 mM), 4 μl of 1 mM ATP, and 20 units of terminal transferase. The reaction mixture was incubated for 15 min at 37 °C and was diluted to 500 μl using 1× Tris-EDTA buffer. The first round of amplification was performed using primers HC03, HC04, and HC02 (an outer *rbn*-specific primer), followed by the second round of amplification using primers HC03 and HC01 (an inner *rbn*-specific primer). PCR products were resolved in a 1.5% agarose gel and were recovered using QIAquick® gel-extraction kit. Purified DNA fragments were ligated with PCR^{TM} 2.1 vector and were sequenced by Genewiz.

Northern blotting

Northern blot analysis was performed by fractionating 15 μg of RNA on 6% polyacrylamide, 7.5 M urea gels. RNA was then transferred onto nylon membranes by the semi-dry transfer method. The fixed membranes were first probed for 5S RNA using the probe 5′-ATGCCTGGCAGTTCCCTACTCTCGC-3′. Membranes were stripped and reprobed for GcvB using the probe 5′-CGGTGCTACATTAATCACTATGGAC-3′. Both probes were 5′-end–labeled using [γ-^{32}P]ATP and T4 polynucleotide kinase. The blots were visualized using a STORM 840 phosphorimaging device. ImageQuant software was used to quantify the bands.

Measurement of RNase BN stability

Overnight cultures were diluted 1:200 into fresh YT medium and grown to exponential phase (A_{600} = 0.4) or stationary phase (A_{600} = 2.0), followed by the treatment with 400 μg/ml chloramphenicol. Equal amounts of cells were removed at different time points as indicated in the figure legends. Changes in RNase BN levels were determined by immunoblotting.

Immunoblotting

Total protein was prepared as described previously (38). Protein concentration was measured by the Bradford assay (39). Equal amounts of protein were separated by 10% SDS-polyacrylamide gels for RNase BN assay or by 15% SDS-polyacrylamide gels for Hfq assay and transferred onto nitrocellulose membranes. Membranes were treated with 3% nonfat milk and incubated with anti-FLAG M2 mAbs (1:1,000 dilution). RNases BN and Hfq were detected with HRP-conjugated anti-mouse IgG antibody and visualized with ECL solutions. Underexposed films were used for quantification using ImageQuant software.

Construction, expression, and purification of RNase E and Hfq

DNA fragments encoding Hfq and the N-terminal domain of RNase E(1–498) were amplified from chromosomal DNA of the WT strain using primers listed in Table S1. PCR products were digested and ligated into the NdeI and BamH I restriction sites of the pET15b expression vector. The constructs were introduced into *E. coli* strain BL21 (DE3) to overexpress His-tagged Hfq and RNase E proteins.

Overnight cultures were diluted 1:100 into 500 ml of YT medium and grown to A_{600} = 0.4 at 37 °C. Overexpression of Hfq and RNase E were induced for 3 h using 1 mM isopropyl 1-thio-β-D-galactopyranoside. Cultures were harvested by centrifugation, followed by protein purification as described in previous work (40) using buffer QE (20 mM Tris-Cl, pH 7.5, 500 mM NaCl, 10% glycerol, 1 mM phenylmethylsulfonyl fluoride). Eluted proteins in buffer QE containing 300 mM imidazole were filtered through Amicon® ultracentrifugal units to remove imidazole and to concentrate.

Substrate preparation

Templates for *in vitro* transcription of *rbn* fragment (1–165) and for GcvB were amplified by PCR from genomic DNA of the WT strain using primers listed in Table S1, followed by gel purification using the QIAquick® gel-extraction kit. *In vitro* transcription was performed according to instructions provided with the MEGAshortscript^{TM} T7 transcription kit using 100 nM template. The two transcripts were purified by extracting the reaction mixture once with phenol/chloroform (1:1) and were precipitated overnight with ethanol at −20 °C. The 5′ terminus of purified *rbn* mRNA was labeled using [γ-^{32}P]ATP and T4 polynucleotide kinase after treatment with calf intestinal alkaline phosphatase.

Gel-shift assay

GcvB and 5′-labeled *rbn* fragment (1–165) were denatured at 95 °C for 2 min, cooled on ice, followed by incubation at 37 °C for 10 min in 1× binding assay buffer (10 mM Tris, pH 7.0, 100 mM KCl, 10 mM $MgCl_2$). For all of the binding reactions (10 μl), 0.1 pmol of *rbn* was added to tubes containing different amounts of GcvB. Purified Hfq (10 pmol) was subsequently added, as needed. The mixture was incubated at 37 °C for 20 min. To determine whether the continued presence of Hfq was required for maintaining the complexes, 10 μg of proteinase K was used to remove Hfq. To examine interaction of *rbn* with GcvB in absence of Hfq, 1 pmol of *rbn* was incubated with increasing amounts of GcvB as indicated in figure legends. The reaction mixtures treated with proteinase K were extracted with phenol/chloroform (1:1) before mixing with 1 μl of native loading dye (50% glycerol, 0.01% bromphenol blue). Other reac-

tion mixtures were directly mixed with 1 μl of native loading dye. The mixtures were separated on a 5% native polyacrylamide gel. Electrophoresis was performed in 0.5× TBE at 200 V in a cold room for 2 h. Gels were subsequently analyzed using a STORM 840 phosphorimaging device.

Primer extension analysis

To identify cleavage sites of RNase E, 0.6 pmol of unlabeled *rbn* mRNA(1–165) was cleaved with purified RNase E at 37 °C using 1× reaction buffer (10 mM Tris-Cl, pH 7.0, 100 mM KCl, 10 mM $MgCl_2$). Samples (60 μl) were removed at different time points as indicated in the figure legends, followed by extraction with phenol/chloroform (1:1) and precipitation with ethanol. Primer HC20 (listed in Table S1) was 5′-end–labeled using [γ-^{32}P]ATP and T4 polynucleotide kinase. Labeled primer was used for both the sequencing reactions and primer-extension analysis. Cleavage products were mixed with labeled primer and dNTPs, heated to 80 °C for 5 min, and slowly cooled to 42 °C, followed by addition of 2 μl of 10× reaction buffer and 10 units of avian myeloblastosis virus–reverse transcriptase. Samples were incubated at 42 °C for 1 h, and reactions were terminated by addition of 20 μl of stop solution (95% formamide, 20 mM EDTA, 0.05% bromphenol, 0.05% xylene cyanol FF). The sequencing reactions were performed according to the instructions in the Thermo Sequence Cycle sequencing kit. Samples were resolved on 8% polyacrylamide, 7.5 M urea gels in parallel with sequencing reaction samples, subsequently dried using the model 583 gel dryer (Bio-Rad), and analyzed using a STORM 840 phosphorimaging device.

RNase E cleavage assay

To identify the cleavage sites that are closer to 5′ end of *rbn* mRNA, 0.6 pmol of 5′-labeled *rbn* fragment (1–165) was cleaved with purified RNase E. To determine whether GcvB and Hfq protect *rbn* mRNA from RNase E cleavage, 5 pmol of GcvB and 60 pmol of Hfq protein were used. The reaction mixture lacking RNase E was incubated for 20 min at 37 °C, followed by addition of RNase E and additional incubation for 15 min. Reaction mixtures (60 μl) were purified by extraction with phenol/chloroform (1:1) and precipitation with ethanol. The cleavage products dissolved in diethyl pyrocarbonate/water were mixed with an equal volume of 2× loading buffer (95% formamide, 20 mM EDTA, 0.05% bromphenol, and 0.05% xylene cyanol FF). The mixtures were resolved on an 8% polyacrylamide, 7.5 M urea gel. After electrophoresis, gels were dried using the model 583 gel dryer (Bio-Rad) and were analyzed using a STORM 840 phosphorimaging device.

Prediction of interaction between sRNAs and rbn mRNA

The list of Hfq-dependent small RNAs was from published data (41). The interaction between sRNAs and *rbn* mRNA was predicted by IntaRNA (20) using the sequences of sRNAs obtained from the BSRD database (42) and the complete sequence of *rbn* mRNA.

Author contributions—H. C. data curation; H. C. and A. P. methodology; M. P. D. conceptualization; M. P. D. supervision; M. P. D. writing-original draft; M. P. D. project administration.

Acknowledgments—We thank Dr. Arun Malhotra and members of the laboratory for critical comments on the manuscript.

References

1. Deutscher, M. P. (2015) Twenty years of bacterial RNases and RNA processing: how we've matured. *RNA* **21,** 597–600 CrossRef Medline
2. Mohanty, B. K., and Kushner, S. R. (2018) Enzymes involved in posttranscriptional RNA metabolism in Gram-negative bacteria. *Microbiol. Spectr.* **6,** CrossRef Medline
3. Deutscher, M. P. (2015) How bacterial cells keep ribonucleases under control. *FEMS Microbiol. Rev.* **39,** 350–361 CrossRef Medline
4. Song, L., Wang, G., Malhotra, A., Deutscher, M. P., and Liang, W. (2016) Reversible acetylation on Lys501 regulates the activity of RNase II. *Nucleic Acids Res.* **44,** 1979–1988 CrossRef Medline
5. Liang, W., Malhotra, A., and Deutscher, M. P. (2011) Acetylation regulates the stability of a bacterial protein: growth stage-dependent modification of RNase R. *Mol. Cell* **44,** 160–166 CrossRef Medline
6. Bárria, C., Pobre, V., Bravo, A. M., and Arraiano, C. M. (2016) in *Stress and Environmental Regulation of Gene Expression and Adaptation in Bacteria* (Bruijn, F. J. D., ed) pp. 174–184, Wiley-Blackwell, Hoboken, NJ
7. Dutta, T., and Deutscher, M. P. (2009) Catalytic properties of RNase BN/RNase Z from *Escherichia coli*: RNase BN is both an exo- and endoribonuclease. *J. Biol. Chem.* **284,** 15425–15431 CrossRef Medline
8. Ezraty, B., Dahlgren, B., and Deutscher, M. P. (2005) The RNase Z homologue encoded by *Escherichia coli* elaC gene is RNase BN. *J. Biol. Chem.* **280,** 16542–16545 CrossRef Medline
9. Dutta, T., Malhotra, A., and Deutscher, M. P. (2012) Exoribonuclease and endoribonuclease activities of RNase BN/RNase Z both function *in vivo*. *J. Biol. Chem.* **287,** 35747–35755 CrossRef Medline
10. Asha, P. K., Blouin, R. T., Zaniewski, R., and Deutscher, M. P. (1983) Ribonuclease BN: identification and partial characterization of a new tRNA processing enzyme. *Proc. Natl. Acad. Sci. U.S.A.* **80,** 3301–3304 CrossRef Medline
11. Seidman, J. G., Schmidt, F. J., Foss, K., and McClain, W. H. (1975) A mutant of *Escherichia coli* defective in removing 3′-terminal nucleotides from some transfer RNA precursor molecules. *Cell* **5,** 389–400 CrossRef Medline
12. Dutta, T., Malhotra, A., and Deutscher, M. P. (2013) How a CCA sequence protects mature tRNAs and tRNA precursors from action of the processing enzyme RNase BN/RNase Z. *J. Biol. Chem.* **288,** 30636–30644 CrossRef Medline
13. Chen, H., Dutta, T., and Deutscher, M. P. (2016) Growth phase-dependent variation of RNase BN/Z affects small RNAs: regulation of 6S RNA. *J. Biol. Chem.* **291,** 26435–26442 CrossRef Medline
14. Gama-Castro, S., Salgado, H., Santos-Zavaleta, A., Ledezma-Tejeida, D., Muñiz-Rascado, L., García-Sotelo, J. S., Alquicira-Hernández, K., Martínez-Flores, I., Pannier, L., Castro-Mondragón, J. A., Medina-Rivera, A., Solano-Lira, H., Bonavides-Martínez, C., Pérez-Rueda, E., Alquicira-Hernández, S., *et al.* (2016) RegulonDB version 9.0: high-level integration of gene regulation, coexpression, motif clustering and beyond. *Nucleic Acids Res.* **44,** D133–D143 CrossRef Medline
15. Thomason, M. K., Bischler, T., Eisenbart, S. K., Förstner, K. U., Zhang, A., Herbig, A., Nieselt, K., Sharma, C. M., and Storz, G. (2015) Global transcriptional start site mapping using differential RNA sequencing reveals novel antisense RNAs in *Escherichia coli*. *J. Bacteriol.* **197,** 18–28 CrossRef Medline
16. Cao, G. J., and Sarkar, N. (1992) Identification of the gene for an *Escherichia coli* poly(A) polymerase. *Proc. Natl. Acad. Sci. U.S.A.* **89,** 10380–10384 CrossRef Medline
17. Kushner, S. R. (2015) Polyadenylation in *E. coli*: a 20-year odyssey. *RNA* **21,** 673–674 CrossRef Medline
18. Deana, A., Celesnik, H., and Belasco, J. G. (2008) The bacterial enzyme RppH triggers messenger RNA degradation by 5′ pyrophosphate removal. *Nature* **451,** 355–358 CrossRef Medline

19. Kavita, K., de Mets, F., and Gottesman, S. (2018) New aspects of RNA-based regulation by Hfq and its partner sRNAs. *Curr. Opin. Microbiol.* **42,** 53–61 CrossRef Medline
20. Mann, M., Wright, P. R., and Backofen, R. (2017) IntaRNA 2.0: enhanced and customizable prediction of RNA–RNA interactions. *Nucleic Acids Res.* **45,** W435–W439 CrossRef Medline
21. Lalaouna, D., Eyraud, A., Devinck, A., Prévost, K., and Massé, E. (2019) GcvB small RNA uses two distinct seed regions to regulate an extensive targetome. *Mol. Microbiol.* **111,** 473–486 CrossRef Medline
22. Ali Azam, T., Iwata, A., Nishimura, A., Ueda, S., and Ishihama, A. (1999) Growth phase-dependent variation in protein composition of the *Escherichia coli* nucleoid. *J. Bacteriol.* **181,** 6361–6370 Medline
23. Cech, G. M., Szalewska-Pałasz, A., Kubiak, K., Malabirade, A., Grange, W., Arluison, V., and Węgrzyn, G. (2016) The *Escherichia coli* Hfq protein: an unattended DNA-transactions regulator. *Front. Mol. Biosci.* **3,** 36 CrossRef Medline
24. Argaman, L., Hershberg, R., Vogel, J., Bejerano, G., Wagner, E. G., Margalit, H., and Altuvia, S. (2001) Novel small RNA-encoding genes in the intergenic regions of *Escherichia coli*. *Curr. Biol.* **11,** 941–950 CrossRef Medline
25. Liang, W., and Deutscher, M. P. (2010) A novel mechanism for ribonuclease regulation: transfer-messenger RNA (tmRNA) and its associated protein SmpB regulate the stability of RNase R. *J. Biol. Chem.* **285,** 29054–29058 CrossRef Medline
26. Dutta, T., and Srivastava, S. (2018) Small RNA-mediated regulation in bacteria: a growing palette of diverse mechanisms. *Gene* **656,** 60–72 CrossRef Medline
27. Papenfort, K., and Vanderpool, C. K. (2015) Target activation by regulatory RNAs in bacteria. *FEMS Microbiol. Rev.* **39,** 362–378 CrossRef Medline
28. Cavanagh, A. T., and Wassarman, K. M. (2014) 6S RNA, a global regulator of transcription in *Escherichia coli*, *Bacillus subtilis*, and beyond. *Annu. Rev. Microbiol.* **68,** 45–60 CrossRef Medline
29. Miyakoshi, M., Chao, Y., and Vogel, J. (2015) Cross talk between ABC transporter mRNAs via a target mRNA-derived sponge of the GcvB small RNA. *EMBO J.* **34,** 1478–1492 CrossRef Medline
30. Sharma, C. M., Papenfort, K., Pernitzsch, S. R., Mollenkopf, H. J., Hinton, J. C., and Vogel, J. (2011) Pervasive post-transcriptional control of genes involved in amino acid metabolism by the Hfq-dependent GcvB small RNA. *Mol. Microbiol.* **81,** 1144–1165 CrossRef Medline
31. Melamed, S., Peer, A., Faigenbaum-Romm, R., Gatt, Y. E., Reiss, N., Bar, A., Altuvia, Y., Argaman, L., and Margalit, H. (2016) Global mapping of small RNA-target interactions in bacteria. *Mol. Cell* **63,** 884–897 CrossRef Medline
32. Pulvermacher, S. C., Stauffer, L. T., and Stauffer, G. V. (2009) Role of the *Escherichia coli* Hfq protein in GcvB regulation of oppA and dppA mRNAs. *Microbiology* **155,** 115–123 CrossRef Medline
33. Datsenko, K. A., and Wanner, B. L. (2000) One-step inactivation of chromosomal genes in *Escherichia coli* K-12 using PCR products. *Proc. Natl. Acad. Sci. U.S.A.* **97,** 6640–6645 CrossRef Medline
34. Jain, C. (1993) New improved lacZ gene fusion vectors. *Gene* **133,** 99–102 CrossRef Medline
35. Miller, J. H. (1972) *Experiments in Molecular Genetics*, pp. 352–355, Cold Spring Harbor Laboratory Press, Cold Spring Harbor, NY
36. Beckmann, B. M., Grünweller, A., Weber, M. H., and Hartmann, R. K. (2010) Northern blot detection of endogenous small RNAs (approximately 14 nt) in bacterial total RNA extracts. *Nucleic Acids Res.* **38,** e147 CrossRef Medline
37. Scotto-Lavino, E., Du, G., and Frohman, M. A. (2006) 5′ end cDNA amplification using classic RACE. *Nat. Protoc.* **1,** 2555–2562 CrossRef Medline
38. Wassarman, K. M., and Storz, G. (2000) 6S RNA regulates *E. coli* RNA polymerase activity. *Cell* **101,** 613–623 CrossRef Medline
39. Bradford, M. M. (1976) A rapid and sensitive method for the quantitation of microgram quantities of protein utilizing the principle of protein-dye binding. *Anal. Biochem.* **72,** 248–254 CrossRef Medline
40. Moll, I., Afonyushkin, T., Vytvytska, O., Kaberdin, V. R., and Bläsi, U. (2003) Coincident Hfq binding and RNase E cleavage sites on mRNA and small regulatory RNAs. *RNA* **9,** 1308–1314 CrossRef Medline
41. Bilusic, I., Popitsch, N., Rescheneder, P., Schroeder, R., and Lybecker, M. (2014) Revisiting the coding potential of the *E. coli* genome through Hfq co-immunoprecipitation. *RNA Biol.* **11,** 641–654 CrossRef Medline
42. Li, L., Huang, D., Cheung, M. K., Nong, W., Huang, Q., and Kwan, H. S. (2013) BSRD: a repository for bacterial small regulatory RNA. *Nucleic Acids Res.* **41,** D233–D238 CrossRef Medline
43. Kawano, M., Reynolds, A. A., Miranda-Rios, J., and Storz, G. (2005) Detection of 5′- and 3′-UTR-derived small RNAs and cis-encoded antisense RNAs in *Escherichia coli*. *Nucleic Acids Res.* **33,** 1040–1050 CrossRef Medline
44. Douchin, V., Bohn, C., and Bouloc, P. (2006) Down-regulation of porins by a small RNA bypasses the essentiality of the regulated intramembrane proteolysis protease RseP in *Escherichia coli*. *J. Biol. Chem.* **281,** 12253–12259 CrossRef Medline
45. Wassarman, K. M., Repoila, F., Rosenow, C., Storz, G., and Gottesman, S. (2001) Identification of novel small RNAs using comparative genomics and microarrays. *Genes Dev.* **15,** 1637–1651 CrossRef Medline
46. Vogel, J., Bartels, V., Tang, T. H., Churakov, G., Slagter-Jäger, J. G., Hüttenhofer, A., and Wagner, E. G. (2003) RNomics in *Escherichia coli* detects new sRNA species and indicates parallel transcriptional output in bacteria. *Nucleic Acids Res.* **31,** 6435–6443 CrossRef Medline
47. Wang, X., Ji, S. C., Jeon, H. J., Lee, Y., and Lim, H. M. (2015) Two-level inhibition of galK expression by Spot 42: degradation of mRNA mK2 and enhanced transcription termination before the galK gene. *Proc. Natl. Acad. Sci. U.S.A.* **112,** 7581–7586 CrossRef Medline